

# Covalent Inhibitors of *Plasmodium falciparum* Glyceraldehyde 3-Phosphate Dehydrogenase with Antimalarial Activity in Vitro

Gregorio Cullia,<sup>†</sup> Stefano Bruno,<sup>‡</sup> Silvia Parapini,<sup>§</sup> Marilena Margiotta,<sup>‡</sup> Lucia Tamborini,<sup>†</sup> Andrea Pinto,<sup>||</sup> Andrea Galbiati,<sup>†</sup> Andrea Mozzarelli,<sup>‡</sup> Marco Persico,<sup>⊥</sup> Antonella Paladino,<sup>#</sup> Caterina Fattorusso,<sup>\*,⊥</sup> Donatella Taramelli,<sup>∇</sup> and Paola Conti<sup>\*,†</sup>

<sup>†</sup>Dipartimento di Scienze Farmaceutiche, Università degli Studi di Milano, Via Mangiagalli 25, 20133 Milano, Italy

<sup>‡</sup>Dipartimento di Scienze degli Alimenti e del Farmaco, Università degli Studi di Parma, Area Parco delle Scienze 23A, 43124 Parma, Italy

<sup>§</sup>Dipartimento di Scienze Biomediche, Chirurgiche e Odontoiatriche, Università degli Studi di Milano, Via Pascal 36, 20133 Milano, Italy

<sup>||</sup>Dipartimento di Scienze per gli Alimenti, la Nutrizione e l'Ambiente, Via Celoria 2, 20133 Milano, Italy

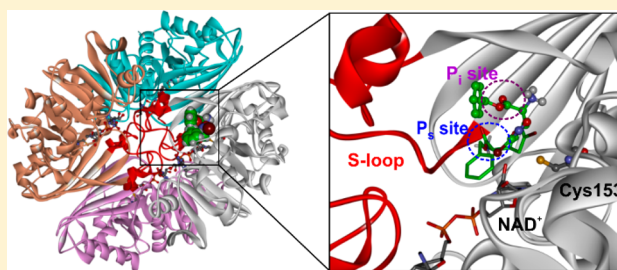
<sup>⊥</sup>Dipartimento di Farmacia, Università degli Studi di Napoli Federico II, Via D. Montesano 49, 80131 Napoli, Italy

<sup>#</sup>Istituto di Chimica del Riconoscimento Molecolare, Consiglio Nazionale delle Ricerche, Via M. Bianco 9, 20131 Milano, Italy

<sup>∇</sup>Dipartimento di Scienze Farmacologiche e Biomolecolari, Università degli Studi di Milano, Via Pascal 36, 20133 Milano, Italy

## Supporting Information

**ABSTRACT:** Covalent inhibitors of *Pf*GAPDH characterized by a 3-bromoisoxazoline warhead were developed, and their mode of interaction with the target enzyme was interpreted by means of molecular modeling studies: some of them displayed a submicromolar antiplasmodial activity against both chloroquine sensitive and resistant strains of *Plasmodium falciparum*, with good selectivity indices.



**KEYWORDS:** Glyceraldehyde 3-phosphate dehydrogenase, malaria, covalent inhibitor, 3-bromoisoxazoline

Malaria, caused by protozoan parasites of the genus *Plasmodium*, is a major human health burden, with almost half of the world population at risk.<sup>1</sup> Efforts to control malaria have been hampered by the lack of an effective vaccine, by the constant resurgence of drug-resistant parasites and by the development of insecticide resistance by mosquito vectors. Therefore, novel therapeutic targets and drugs are urgently needed.<sup>2</sup>

It is well established that *P. falciparum* solely depends on glycolysis for energy generation and fulfills its energy needs by anaerobic metabolism of glucose since both the parasite and red blood cells are devoid of a functional Krebs cycle.<sup>3</sup> As a result, the rate of glycolysis in *P. falciparum*-infected erythrocytes is 20–100 times higher than in uninfected erythrocytes.<sup>4,5</sup> Therefore, compounds targeting the parasite ATP-generating machinery could be potential antimalarials. Particularly, glyceraldehyde-3-phosphate dehydrogenase (GAPDH) is a key glycolytic enzyme that catalyzes the oxidation of glyceraldehyde-3-phosphate (G3P) to 1,3-biphosphoglycerate (1,3-BPG), coupled to the reduction of nicotinamide adenine dinucleotide (NAD<sup>+</sup>) to NADH.<sup>6</sup> Moreover, it has been demonstrated that *Plasmodium* sporozoite GAPDH, expressed on the surface of *Plasmodium*

sporozoites, binds to CD68, a ligand critical for Kupffer cell traversal and liver infection.<sup>7</sup> The gene for *P. falciparum* GAPDH (*Pf*GAPDH) has been cloned, and the three-dimensional structure of the protein, expressed in *Escherichia coli*, has been determined by X-ray diffraction.<sup>8</sup> The enzyme is a homotetramer, and the catalytic mechanism relies on the intervention of a cysteine residue, activated by a histidine residue (Cys153 and His180 in *Pf*GAPDH, respectively) (Figure 1SI): the generated thiolate reacts with G3P, giving a thioester intermediate and reducing the NAD<sup>+</sup> cofactor; the subsequent phosphorolysis releases 1,3-BPG.<sup>9–11</sup>

In recent years, we have shown that the 3-bromoisoxazoline ring can serve as an efficient warhead able to irreversibly react with Cys residues within the catalytic site of different classes of enzymes.<sup>12</sup> Thus, enzymatic inhibitors can be designed by coupling the 3-Br-isoxazoline nucleus to a proper recognition

**Special Issue:** Highlighting Medicinal Chemistry in Italy

**Received:** November 29, 2018

**Accepted:** February 20, 2019

**Published:** February 20, 2019

moiety, able to selectively interact with a specific binding pocket.

In a previous work, we have reported that a series of 3-Br-isoxazoline derivatives were able to selectively react with the catalytic Cys153 of *Pf*GAPDH, as demonstrated by mass spectrometry.<sup>13</sup> Their inhibition efficiency was related to the substitution pattern on the isoxazoline ring.<sup>13</sup> Very interestingly, whereas *Pf*GAPDH was fully and irreversibly inactivated, the human ortholog was only 25% inhibited.<sup>14</sup>

Based on these results, we expanded the structure–activity relationship (SAR) studies around the more promising chemical scaffold, exemplified by the general structure A<sup>I</sup>, generating new derivatives of general structure A<sup>II</sup>, A<sup>III</sup>, and A<sup>IV</sup> (Chart 1). It must be underlined that 3-Br-Acivicin

Chart 1. Molecular Structure of the Compounds under Study

Compd	Scaffold	R	X
( $\alpha$ S, $\alpha$ S)-1a	A <sup>I</sup>	H	-
( $\alpha$ S, $\alpha$ S)-1b	A <sup>I</sup>	CH <sub>3</sub> -	-
( $\alpha$ S, $\alpha$ S)-1c	A <sup>I</sup>	PhCH <sub>2</sub> -	-
( $\alpha$ S, $\alpha$ S)-2a	A <sup>II</sup>	PhCH <sub>2</sub> -	-
( $\alpha$ S, $\alpha$ S)-2b	A <sup>II</sup>	<i>p</i> -MeO-PhCH <sub>2</sub> -	-
( $\alpha$ S, $\alpha$ S)-2c	A <sup>II</sup>	<i>p</i> -F-PhCH <sub>2</sub> -	-
( $\alpha$ S, $\alpha$ S)-2d	A <sup>II</sup>	<i>p</i> -NO <sub>2</sub> -PhCH <sub>2</sub> -	-
( $\alpha$ S, $\alpha$ S)-2e	A <sup>II</sup>	PhCH <sub>2</sub> CH <sub>2</sub> -	-
( $\alpha$ R, $\alpha$ S)-3a	A <sup>III</sup>	PhCH <sub>2</sub> -	O
( $\alpha$ S, $\alpha$ S)-3b	A <sup>III</sup>	PhCH <sub>2</sub> -	S
( $\alpha$ S, $\alpha$ S)-3c	A <sup>III</sup>	PhCH <sub>2</sub> -	SO <sub>2</sub>
( $\alpha$ S, $\alpha$ SR)-4b	A <sup>IV</sup>	PhCH <sub>2</sub> -	S
( $\alpha$ S, $\alpha$ SR)-4c	A <sup>IV</sup>	PhCH <sub>2</sub> -	SO <sub>2</sub>

(compound 1a, Chart 1) was previously shown to covalently inhibit also the family of L-glutamine-dependent amidotransferases, due to its structural similarity with glutamine.<sup>15,16</sup> Therefore, its structure was elaborated to lose the glutamine-mimicking character, by modifying the amino acidic portion.

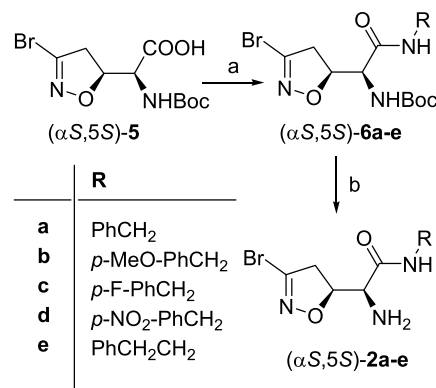
All the compounds under study are characterized by a 5-substituted 3-Br-isoxazoline scaffold, which can be generated exploiting the well-described 1,3-dipolar cycloaddition reaction of bromonitrile oxide to suitable dipolarophiles.<sup>17</sup> The synthesis of compounds ( $\alpha$ S, $\alpha$ S)-1a–c was previously described by us,<sup>13</sup> as well as the synthesis of key intermediate ( $\alpha$ S, $\alpha$ S)-5,<sup>15</sup> used to obtain all derivatives of general structure A<sup>II</sup>.

Carboxylic acid ( $\alpha$ S, $\alpha$ S)-5 was transformed into the corresponding amide derivatives by standard coupling reaction with the desired amines, using *N*-(3-(dimethylamino)propyl)-*N'*-ethylcarbodiimide hydrochloride (EDC·HCl) and hydrox-

ybenzotriazole (HOBt) as coupling reagents, in dry tetrahydrofuran (THF).

Intermediates ( $\alpha$ S, $\alpha$ S)-6a–e were then converted into derivatives ( $\alpha$ S, $\alpha$ S)-2a–e by standard *N*-Boc deprotection with a 15% solution of trifluoroacetic acid (TFA) in dichloromethane (DCM) (Scheme 1). The ether derivative

Scheme 1. Synthesis of Compounds 2a–e<sup>a</sup>



<sup>a</sup>Reagents and conditions: (a) RNH<sub>2</sub>, EDC·HCl, HOBt, dry THF, rt; (b) 15% TFA/DCM, rt.

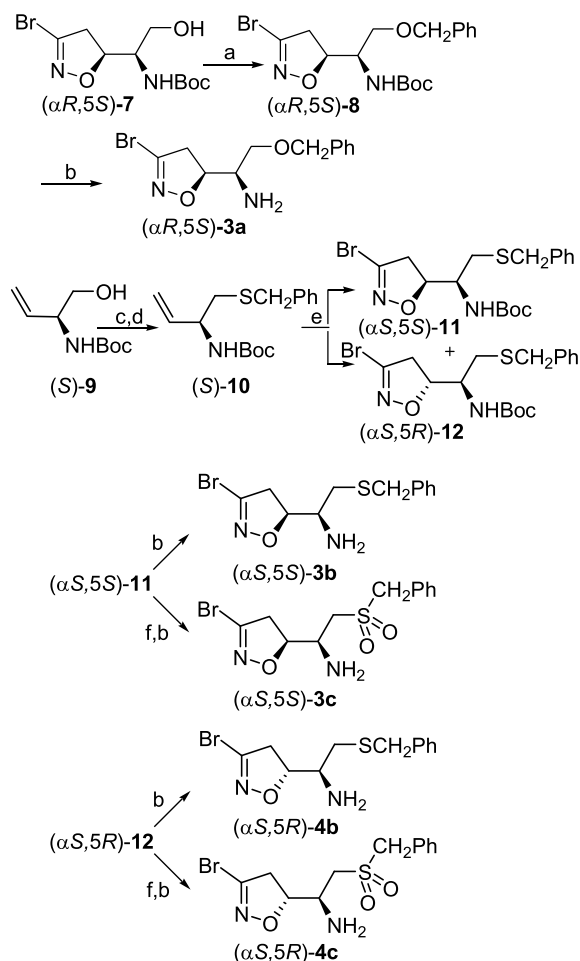
( $\alpha$ R, $\alpha$ S)-3a was obtained starting from another previously described synthetic intermediate, alcohol ( $\alpha$ R, $\alpha$ S)-7,<sup>15</sup> which was treated with benzyl bromide, in the presence of silver(I) oxide in dry DCM to afford ( $\alpha$ R, $\alpha$ S)-8, which was then deprotected by standard treatment with a 15% solution of TFA in DCM (Scheme 2).

Finally, to generate compounds ( $\alpha$ S, $\alpha$ S)-3b and ( $\alpha$ S, $\alpha$ S)-3c (Scheme 2), we started from alkene (*S*)-9, prepared according to a literature procedure starting from (*S*)-Garner's aldehyde.<sup>18</sup> Alkene (*S*)-9 was converted into the corresponding mesylate and then treated with benzyl mercaptan in the presence of 1,8-diazabicyclo[5.4.0]undec-7-ene (DBU) to afford the thioether (*S*)-10. The latter was submitted to 1,3-dipolar cycloaddition reaction with bromonitrile oxide, slowly generated in situ by dehydrohalogenation of the stable precursor dibromoformal-doxime (DBF), in a heterogeneous mixture of NaHCO<sub>3</sub> in ethyl acetate. The pericyclic reaction produced a diastereomeric mixture of *erythro* ( $\alpha$ S, $\alpha$ S)-11 and *threo* ( $\alpha$ S, $\alpha$ SR)-12 in a 45:55 ratio, which were separated by flash chromatography.

Intermediate ( $\alpha$ S, $\alpha$ S)-11 was either converted into the corresponding amine ( $\alpha$ S, $\alpha$ S)-3b, by standard *N*-Boc deprotection or was first oxidized with *meta*-chloroperbenzoic acid (*m*-CPBA) and then deprotected to afford sulfone derivative ( $\alpha$ S, $\alpha$ S)-3c. The same procedure, carried out on the *threo* isomer ( $\alpha$ S, $\alpha$ SR)-12, afforded the thioether derivative ( $\alpha$ S, $\alpha$ SR)-4b or the sulfone ( $\alpha$ S, $\alpha$ SR)-4c.

The derivatives under study produced a time- and concentration-dependent inhibition of *Pf*GAPDH (Table 1), suggesting irreversible inhibition, as already evidenced for the previous series.<sup>13</sup> The resulting Kitz–Wilson  $k_{\text{inact}}/K_i$  ratios are reported in Table 1 (higher values indicate higher inhibition).<sup>19</sup>

To rationalize the outcome of the biochemical assays, computational studies were performed. First, the molecular models of the compounds in Chart 1 were subjected to conformational analysis. Then, the low energy conformers of 1b, 1c, 2a, and 3c ( $\Delta E_{\text{GM}} \leq 5$  kcal/mol) were placed in the *Pf*GAPDH catalytic site (PDB ID: 1YWG) to perform docking

Scheme 2. Synthesis of Compounds 3a–c and 4b–c<sup>a</sup>

<sup>a</sup>Reagents and conditions: (a) PhCH<sub>2</sub>Br, Ag<sub>2</sub>O, dry DCM, rt; (b) 15% TFA/DCM; (c) MsCl, TEA, DMAP, dry DCM, 0 °C; (d) PhCH<sub>2</sub>SH, DBU, benzene, rt; (e) i. DBF, NaHCO<sub>3</sub>, EtOAc, rt. ii. chromatographic separation; (f) mCPBA, CHCl<sub>3</sub>, rt.

studies. The aim was to mimic the approach of the compounds to the catalytic Cys153, just before undergoing the nucleophilic attack. Experimental evidence reported that the substrate assumes two binding modes during the catalysis (Figure 1SI), shifting the phosphate from the P<sub>i</sub> site to the P<sub>s</sub> site through a flip-flop mechanism, which involves the S-loop (residues 181–209) and also allows NAD<sup>+</sup>/NADH exchange.<sup>20,21</sup> Accordingly, two possible binding approaches to Cys153 were considered for each compound by placing the H-bond forming groups of the linker (ester, amide, or sulfone) at the P<sub>i</sub> or the P<sub>s</sub> site.

The starting complexes were then subjected to dynamic docking simulation by applying a MonteCarlo/Metropolis-based procedure, considering the whole system (i.e., ligand and protein) as flexible (for details see the SI). Since the catalytic cysteine must be activated in order to react, a tethering restraint was applied on the hydrogen bond between Cys153 and His180. Moreover, the distance between the electrophilic carbon of the 3-Br-isoxazoline ring and the sulfur atom of Cys153 was restrained to a maximum of 3.4 Å, the limit distance to allow a nucleophilic attack.<sup>22,23</sup> At the end of the docking procedure, in order to allow the relaxation of the whole structure, the selected docked complexes were subjected to Molecular Mechanics energy minimization without any restraint. For each docking calculation, the complex with the best nonbonded interaction energy was selected (Tables 1–SSI).

Compound 1b ( $k_{\text{inact}}/K_i = 10.7 \text{ s}^{-1} \text{ M}^{-1}$ ), which presents the less hindered substituent, is able to properly orient with respect to Cys153 either approaching from the P<sub>i</sub> or from the P<sub>s</sub> site (Figure 2SIA,B). In the first case, with the ester group binding at the P<sub>i</sub> site, 1b is characterized by the most favorable binding energy (Table 6SI), with the protonated amine function establishing hydrogen bonds with Thr154 and Gly215 and the methyl ester group reproducing the position of the substrate phosphate group at the P<sub>i</sub> site (Figure 2SIA). This is confirmed by the fact that this binding mode is preserved also after the unrestrained energy minimization. Instead, when the ester group is placed at the P<sub>s</sub> site, 1b “slips away” from the original binding region toward the exterior of the protein, due to the limited size of the methyl substituent with respect to the

Table 1. Kitz–Wilson Parameter on PfGAPDH, Cytotoxicity against *P. falciparum* D10 and W2 Strains, Cytotoxicity against HMEC-1 Cells, and cLogD Values of the Compounds under Study

	PfGAPDH $k_{\text{inact}}/K_i$ (s <sup>-1</sup> M <sup>-1</sup> ) <sup>a</sup>	D10 IC <sub>50</sub> (μM) <sup>a</sup>	W2 IC <sub>50</sub> (μM) <sup>a</sup>	HMEC-1 IC <sub>50</sub> (μM) <sup>b</sup>	SI IC <sub>50</sub> HMEC-1/IC <sub>50</sub> D10	SI IC <sub>50</sub> HMEC-1/IC <sub>50</sub> W2	cLog D <sub>7.4</sub>
1a	0.7	0.35 ± 0.08	0.34 ± 0.12	19.7 ± 6.8	56.3	57.9	0.02
1b	10.7	0.79 ± 0.21	0.88 ± 0.23	34.8 ± 10.4	44.0	39.5	0.04
1c	6.6	0.37 ± 0.12	0.26 ± 0.05	>65	>175.7	>250	1.41
2a	0.6	0.36 ± 0.11	0.48 ± 0.18	14.9 ± 4.3	41.4	31.0	0.76
2b	inact	nd	nd	nd	nd	nd	0.65
2c	inact	nd	nd	nd	nd	nd	0.92
2d	1.9	0.79 ± 0.07	0.72 ± 0.24	36.1 ± 1.2	45.7	50.1	0.80
2e	0.4	0.28 ± 0.09	0.25 ± 0.07	>100	>357	>400	0.97
3a	2.6	inact	inact	nd	nd	nd	0.65
3b	1.6	inact	inact	nd	nd	nd	1.00
3c	inact	nd	nd	nd	nd	nd	0.62
4b	0.2	inact	inact	nd	nd	nd	1.00
4c	1.6	inact	inact	nd	nd	nd	0.62
CQ	nd	0.020 ± 0.005	0.40 ± 0.10	>40	>2000	>100	nd

<sup>a</sup>PLDH method; data are the mean of three different experiments ± SD made in duplicate; D10 CQ-susceptible *Pf* strain; W2, CQ-resistant strain.  
<sup>b</sup>MTT method, data are the mean of three different experiments ± SD made in duplicate; SI selectivity index.

binding pocket (Figure 3SI). However, considering the positioning of the imminent leaving group (the hindered bromine atom), the most favorable orientation is observed with **1b** approaching from the  $P_s$  site (solvent accessible surface area (SASA) of bromine, 24.034 Å<sup>2</sup>, Figure 2SIB, vs bromine SASA, 12.635 Å<sup>2</sup>, Figure 2SIA).

Similar results were obtained for **1c** ( $k_{\text{inact}}/K_i = 6.6 \text{ s}^{-1} \text{ M}^{-1}$ ) characterized by a more hindered phenyl moiety (Figure 1A,B

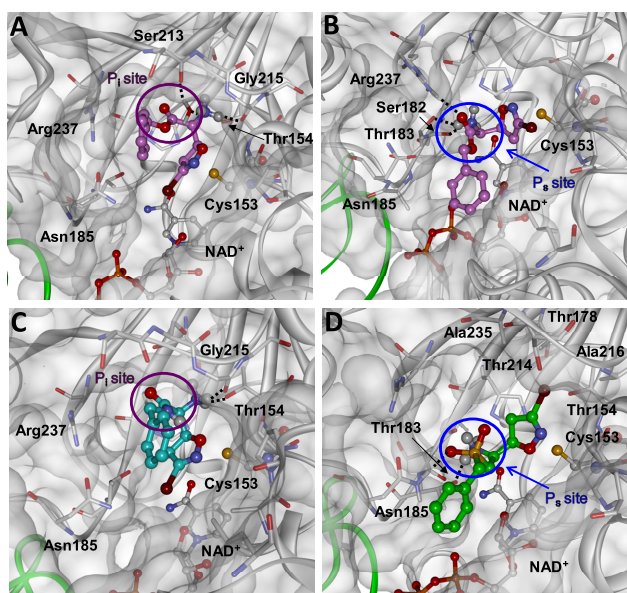


**Figure 1.** Overview of **1c** (pink) bound to  $P_i$  site (A) and  $P_s$  site (B) of *PfGAPDH*. (C) Overview of **2a** (cyan) bound to  $P_i$  site of *PfGAPDH*. (D) Overview of **4c** (green) bound to  $P_s$  site of *PfGAPDH*. The protein (gray) is displayed as Connolly surface and solid ribbons; the second monomer is colored in green. The ligands, NAD<sup>+</sup> and Cys153 (ball and stick), as well as the residues involved in the interactions with ligands (stick) are colored by atom type (N, blue; O, red; P, orange; S, yellow; Br, brown).

vs Figure 2SIA,B), although with some differences. When placing the ester group at the  $P_s$  site, the presence of the phenyl ring, positioned between the S-loop and NAD<sup>+</sup>, stabilizes the ligand binding mode (H-bond with Arg237; Figure 1B), which is preserved even after unrestrained energy minimization. Nevertheless, **1c** presents a less favorable orientation of the (leaving) bromine atom with respect to **1b**, either binding with the ester group at the  $P_i$  (Figure 1A; bromine SASA, 11.194 Å<sup>2</sup>) or at the  $P_s$  (Figure 1B; bromine SASA, 16.130 Å<sup>2</sup>) site. The reduction of the ester function (**1c**) to ether (**3a**) should cause the loss of a favorable interaction with the  $P_s$  site, accounting for its reduced inhibitory activity (Table 1). However, the carboxylic group of **1a** could establish a salt-bridge with Arg237, thus slowing down the alkylation reaction, in agreement with the drastic reduction of the inhibitory activity (Table 1).

When the ester function of **1c** is exchanged for an amide function (**2a**;  $k_{\text{inact}}/K_i = 0.6 \text{ s}^{-1} \text{ M}^{-1}$ ), the isoxazoline ring is able to undergo the nucleophilic attack by Cys153 only with the amide group at the  $P_i$  site (Figure 1C). Indeed, when at the  $P_s$  site, the amide function interacts with a hydroxyl group of NAD<sup>+</sup> shifting the methylene group of the isoxazoline ring in between the electrophilic carbon and Cys153 sulfur atom (Figure 2SIC). Moreover, even when **2a** approaches from the  $P_i$  site, due to an H-bond between the amide function and the

isoxazoline ring, the phenyl group points toward the  $P_s$  site, close to Arg237 and Asn185, reducing the SASA of the bromine atom (3.338 Å<sup>2</sup>; Figure 1C). The SAR of the other amide analogues can be explained combining **2a** docking results with those obtained by the conformational analysis. Compounds **2b** and **2c** showed a complete loss of activity, while **2d** ( $k_{\text{inact}}/K_i = 1.9 \text{ s}^{-1} \text{ M}^{-1}$ ) resulted more active than **2a**. Compounds **2a–d** showed the same families of low energy conformers, including **2a** putative bioactive conformation (which is also present among the low energy conformers of **2e**) ( $k_{\text{inact}}/K_i = 0.4 \text{ s}^{-1} \text{ M}^{-1}$ ). In this view, the nitro group of **2d** could establish favorable interactions with Lys194 (S-loop) (Figure 4SIA), whereas, in the case of **2b**, according to the nature of the substituent, it is likely that the polarization of the phenyl ring is responsible for its lack of activity (Figure 5SI). Finally, the fluorine substituent of **2c**, though able to reproduce the same extra-interaction with the S-loop as the nitro group of **2d** (Figure 4SIB), thanks to its smaller size and its versatile nature as bioisostere, can also promote alternative binding modes at the  $P_i$  site, not compatible with Cys153 alkylation (Figure 6SI).

Docking results obtained for **3c** showed that the introduction of a sulfone function in the linker does not allow the proper orientation with respect to Cys153, neither approaching from the  $P_i$  nor from the  $P_s$  site (Figure 7SI). Indeed, the sulfone function in the  $P_i$  site establishes H-bond interactions with Arg237 pushing the amine toward the catalytic residues His180 and Cys153 (Figure 7SIA). However, in the  $P_s$  site the SO<sub>2</sub> group is H-bonded to Asn185 (S-loop), and the amine function interacts with a phosphate group of NAD<sup>+</sup>; consequently, the bromine atom is placed in between the electrophilic carbon and Cys153 (Figure 7SIB). In this view, the reduction of the sulfone moiety (**3c**) to thioether (**3b**) restored an inhibitory activity similar to that of **3a** (Table 1) due to the removal of the unfavorable interactions mentioned above. Docking studies performed on the ( $\alpha$ S,*SR*)-diastereoisomer of **3c** (i.e., **4c**) showed that, approaching from the  $P_s$  site, the isoxazoline ring is able to properly orient with respect to Cys153 in a similar manner as **1c** (Figure 1D vs B). However, due to its different stereochemistry, **4c** differently positions the bromine atom, strongly reducing its solvent accessibility (SASA, 3.314 Å<sup>2</sup>; Figure 1D). In particular, **4c** places the SO<sub>2</sub> group at  $P_s$  in the same location of the phosphate group of the substrate, establishing H-bond interactions with Asn185 and Thr183. Accordingly, when the ( $\alpha$ S,*SR*)-diastereoisomers **4b** and **4c** were tested, it was found that, whereas the thioether ( $\alpha$ S,*SR*)-**4b** was about 10-times less potent than its diastereoisomer ( $\alpha$ S,*SS*)-**3b**, in the case of the sulfone derivative the trend was inverted and the ( $\alpha$ S,*SR*) diastereoisomer **4c** was significantly more active than the ( $\alpha$ S,*SS*) diastereoisomer **3c**. These results are in agreement with docking studies, which evidenced that, in this new series of diastereoisomers, the sulfone function plays a favorable role in the interaction with *PfGAPDH*.

Taken together, the docking results account for the role played by the different substituents on the isoxazoline ring on *PfGAPDH* inhibition. We can conclude that the presence of an ester function (**1b** and **1c**) allows the binding to both the  $P_i$  and the  $P_s$  site, favoring the release of bromine consistently to the bulk of the R substituent. On the contrary, the introduction of the amide function (**2a**) allows the binding only to the  $P_i$  site slowing down the release of bromine. Finally, the introduction of a sulfone moiety (**3c**) does not allow a binding

mode compatible with the putative alkylation reaction, except when changing the compound stereochemistry, as in **4c**. In all hypothesized binding modes, the S-loop is involved in the interaction with the ligands as well as in the release of the leaving group. The S-loop forms a long ridge that separates the NAD<sup>+</sup> binding cavities of adjacent subunits (Figure 1SI), and it is known that its sequence variation between human and *Pf* GAPDH induces a different functional behavior.<sup>24</sup> Thus, the hypothesized binding modes could also explain the cooperative inhibition mechanism of these compounds<sup>13</sup> as well as their selectivity over human GAPDH.<sup>14</sup>

All the compounds displaying *Pf*GAPDH inhibitory activity were then assayed in vitro for antiparasitic activity. The phenotypic assays were conducted against D10 (chloroquine sensitive) and W2 (chloroquine resistant) strains of *P. falciparum* using the parasite lactate dehydrogenase (pLDH) method and chloroquine (CQ) as control.

As shown in Table 1 and in Figure 8SI, several compounds displayed submicromolar IC<sub>50</sub> against both *P. falciparum* strains with no difference between the D10 and W2 strains. However, there is not a close parallelism between the observed enzymatic inhibitory activity and the antiparasitic effect. This is not due to instability of the compounds in the assay medium, as detailed in the SI. It has to be underlined that a slower reaction rate, especially when compensated by a high binding affinity, does not necessarily correspond to a lower inhibitory effect on *P. falciparum* strains. Indeed, considering that the incubation time of the inhibitor with *P. falciparum* is 72 h and that these inhibitors act through a time-dependent irreversible covalent mechanism, even relatively slow inactivators, as **2e**, may result in very active antiparasitic compounds. However, the inactivity of **3a**, **3b**, **4b**, and **4c** in the phenotypic assays, despite their inhibitory activity against *Pf*GAPDH, may be due to their inability to cross host and/or parasite membranes. Membrane uptake may occur by passive diffusion through the lipid bilayer or transport through channels or carriers.<sup>25</sup> The cLogD values of these compounds are in the range 0.02–1.41, with no correlation with their antiplasmodial activity (Table 1). Interestingly, similar results were previously obtained by us on a different series of antimalarials.<sup>26</sup> Since it is known that a clogD value >1 is required for drug passive diffusion,<sup>27</sup> it cannot be excluded that our compounds utilize some kind of carrier-mediated transport.<sup>28</sup> Considering that all the active derivatives are characterized by the presence of an  $\alpha$ -amino carbonyl group, whereas all the inactive ones (**3a**, **3b**, **4b**, and **4c**) still possess the amino group but are devoid of the carbonyl group, we could speculate that the presence of the carbonyl function may be relevant for the recognition by the putative transporter.

The active compounds were also tested for cytotoxicity against the human endothelial cell line HMEC-1 in a 72 h (3-(4,5-dimethylthiazol-2-yl)-2,5-diphenyl tetrazolium bromide (MTT) assay. All of them were quite safe with selectivity indices (SI) above 30 (Table 1).

Of particular interest is compound **1c**, which is the second most active against *Pf*GAPDH and also one of the most active against both parasite strains, with good selectivity indices (>175–250). Similar potency and increased selectivity is presented by compound **2e**, although the activity against *Pf*GAPDH is 16-times lower than compound **1c**.

At this stage, the possibility that the compounds under study may interact with additional targets and that the inhibition of more than one enzymatic activity may contribute to the

observed antiproliferative effect cannot be ruled out. To clarify this point, a chemo-proteomic study using activity-based probes is in due course.

## ■ ASSOCIATED CONTENT

### Supporting Information

The Supporting Information is available free of charge on the ACS Publications website at DOI: 10.1021/acsmchemlett.8b00592.

Materials and Methods; Figures 1–8 SI; Tables 1–7 SI (PDF)

## ■ AUTHOR INFORMATION

### Corresponding Authors

\*E-mail: [paola.conti@unimi.it](mailto:paola.conti@unimi.it). Phone: (+39) 02-50319329.

\*E-mail: [caterina.fattorusso@unina.it](mailto:caterina.fattorusso@unina.it). Phone: (+39) 081-678544.

### ORCID

Andrea Pinto: 0000-0002-2501-3348

Andrea Mozzarelli: 0000-0003-3762-0062

Paola Conti: 0000-0003-2140-0567

### Author Contributions

All authors have given approval to the final version of the manuscript.

### Funding

This work was supported by MIUR (PRIN 20154JRJPP\_4) and Università degli Studi di Milano (Dotazione annuale per attività istituzionali, Linea 2).

### Notes

The authors declare no competing financial interest.

## ■ ACKNOWLEDGMENTS

This work is dedicated to prof. Carlo De Micheli on the occasion of his retirement.

## ■ ABBREVIATIONS

ATP, adenosine triphosphate; 1,3-BPG, 1,3-biphosphoglycerate; Boc, *tert*-butoxycarbonyl; CQ, chloroquine; DBF, dibromoformaldoxyme; DBU, 1,8-diazabicyclo[5.4.0]undec-7-ene; DCM, dichloromethane; DMAP, 4-(dimethylamino)pyridine; EDC, *N*-(3-(dimethylamino)propyl)-*N'*-ethylcarbodiimide; GAPDH, glyceraldehyde 3-phosphate dehydrogenase; G3P, glyceraldehyde 3-phosphate; HOBt, hydroxybenzotriazole; *m*-CPBA, *meta*-chloroperbenzoic acid; MsCl, methanesulfonyl chloride; MTT, (3-(4,5-dimethylthiazol-2-yl)-2,5-diphenyl tetrazolium bromide; NAD, nicotinamide adenine dinucleotide; pLDH, parasite lactate dehydrogenase; SAR, structure–activity relationship; SI, selectivity index; TEA, trimethylamine; TFA, trifluoroacetic acid; THF, tetrahydrofuran

## ■ REFERENCES

- (1) WHO. Malaria report 2017.
- (2) malERA Refresh Consultative Panel on Basic Science and Enabling Technologies. malERA: An updated research agenda for basic science and enabling technologies in malaria elimination and eradication. *PLoS Med.* 2017, 14 (11), e1002451.
- (3) Alam, A.; Neyaz, K.; Hasan, S. I. Exploiting Unique Structural and Functional Properties of Malarial Glycolytic Enzymes for Antimalarial Drug Development. *Malar. Res. Treat.* 2014, 2014, 451065.

- (4) Pfaller, M. A.; Krogstad, D. J.; Parquette, A. R.; Dinh, P. N. *Plasmodium falciparum*: stage-specific lactate production in synchronized cultures. *Exp. Parasitol.* **1982**, *54*, 391–396.
- (5) Vander Jagt, D. L.; Hunsaker, L. A.; Campos, N. M.; Baack, B. R. d-Lactate production in erythrocytes infected with *Plasmodium falciparum*. *Mol. Biochem. Parasitol.* **1990**, *42*, 277–284.
- (6) Seidler, N. W. GAPDH and intermediary metabolism. *Adv. Exp. Med. Biol.* **2013**, *985*, 37–59.
- (7) Cha, S.; Kim, M.; Pandey, A.; Jacobs-Lorena, M. Identification of GAPDH on the surface of *Plasmodium* sporozoites as a new candidate for targeting malaria liver invasion. *J. Exp. Med.* **2016**, *213*, 2099–2112.
- (8) Satchell, J. F.; Malby, R. L.; Luo, C. S.; Adisa, A.; Alpyurek, A. E.; Klonis, N.; Smith, B. J.; Tilley, L.; Colman, P. M. Structure of glyceraldehyde-3-phosphate dehydrogenase from *Plasmodium falciparum*. *Acta Crystallogr., Sect. D: Biol. Crystallogr.* **2005**, *D61*, 1213–1221.
- (9) Segal, H. L.; Boyer, P. D. The role of sulfhydryl groups in the activity of D-glyceraldehyde 3-phosphate dehydrogenase. *J. Biol. Chem.* **1953**, *204*, 265–281.
- (10) Trentham, D. R. Reactions of D-glyceraldehyde 3-phosphate dehydrogenase facilitated by oxidized nicotinamide-adenine dinucleotide. *Biochem. J.* **1971**, *122*, 59–69.
- (11) Trentham, D. R. Rate-determining processes and the number of simultaneously active sites of D-glyceraldehyde 3-phosphate dehydrogenase. *Biochem. J.* **1971**, *122*, 71–77.
- (12) Pinto, A.; Tamborini, L.; Cullia, G.; Conti, P.; De Micheli, C. Inspired by Nature: The 3-Halo-4,5-dihydroisoxazole Moiety as a Novel Molecular Warhead for the Design of Covalent Inhibitors. *ChemMedChem* **2016**, *11*, 10–14.
- (13) Bruno, S.; Pinto, A.; Paredi, G.; Tamborini, L.; De Micheli, C.; La Pietra, V.; Marinelli, L.; Novellino, E.; Conti, P.; Mozzarelli, A. Discovery of covalent inhibitors of glyceraldehyde-3-phosphate dehydrogenase, a target for the treatment of malaria. *J. Med. Chem.* **2014**, *57*, 7465–7471.
- (14) Bruno, S.; Margiotta, M.; Pinto, A.; Cullia, G.; Conti, P.; De Micheli, C.; Mozzarelli, A. Selectivity of 3-bromo-isoxazoline inhibitors between human and *Plasmodium falciparum* glyceraldehyde 3-phosphate dehydrogenases. *Bioorg. Med. Chem.* **2016**, *24*, 2654–2659.
- (15) Conti, P.; Pinto, A.; Wong, P. E.; Major, L. L.; Tamborini, L.; Iannuzzi, M. C.; De Micheli, C.; Barrett, M. P.; Smith, T. K. Synthesis and in vitro/in vivo evaluation of the antitrypanosomal activity of 3-bromoacivicin, a potent CTP synthetase inhibitor. *ChemMedChem* **2011**, *6*, 329–333.
- (16) Conti, P.; Roda, G.; Stabile, H.; Vanoni, M. A.; Curti, B.; De Amici, M. Synthesis and biological evaluation of new amino acids structurally related to the antitumor agent Acivicin. *Farmaco* **2003**, *58*, 683–690.
- (17) Pinto, A.; Conti, P.; De Amici, M.; Tamborini, L.; Madsen, U.; Nielsen, B.; Christesen, T.; Brauner-Osborne, H.; De Micheli, C. Synthesis and pharmacological characterization at glutamate receptors of the four enantiopure isomers of tricholomic acid. *J. Med. Chem.* **2008**, *51*, 2311–2315.
- (18) Daniels, R. N.; Melancon, B. J.; Wang, E. A.; Crews, B. C.; Marnett, L. J.; Sulikowski, G. A.; Lindsley, C. W. Progress toward the total synthesis of Lucentamycin A: total synthesis and biological evaluation of 8-epi-Lucentamycin A. *J. Org. Chem.* **2009**, *74* (22), 8852–8855.
- (19) Kitz, R.; Wilson, I. B. Esters of methanesulfonic acid as irreversible inhibitors of acetylcholinesterase. *J. Biol. Chem.* **1962**, *237*, 3245–3249.
- (20) Moniot, S.; Bruno, S.; Vonnrhein, C.; Didierjean, C.; Boschi-Muller, S.; Vas, M.; Bricogne, G.; Branlant, G.; Mozzarelli, A.; Corbier, C. Trapping of the thioacylglyceraldehyde-3-phosphate dehydrogenase intermediate from *Bacillus stearothermophilus*. Direct evidence for a flip-flop mechanism. *J. Biol. Chem.* **2008**, *283*, 21693.
- (21) Castilho, M. S.; Pavão, F.; Oliva, G.; Ladame, S.; Willson, M.; Périé, J. Evidence for the two phosphate binding sites of an analogue of the thioacyl intermediate for the *Trypanosoma cruzi* glyceraldehyde-3-phosphate dehydrogenase-catalyzed reaction, from its crystal structure. *Biochemistry* **2003**, *42*, 7143–7151.
- (22) Lodola, A.; Branduardi, D.; De Vivo, M.; Capoferri, L.; Mor, M.; Piomelli, D.; Cavalli, A. A catalytic mechanism for cysteine N-terminal nucleophile hydrolases, as revealed by free energy simulations. *PLoS One* **2012**, *7* (2), No. e32397.
- (23) Arafet, K.; Ferrer, S.; González, F. V.; Moliner, V. Quantum mechanics/molecular mechanics studies of the mechanism of cysteine protease inhibition by peptidyl-2,3-epoxyketones. *Phys. Chem. Chem. Phys.* **2017**, *19*, 12740–12748.
- (24) Robien, M. A.; Bosch, J.; Buckner, F. S.; Van Voorhis, W. C.; Worthey, E. A.; Myler, P.; Mehlin, C.; Boni, E. E.; Kalyuzhniy, O.; Anderson, L.; Lauricella, A.; Gulde, S.; Luft, J. R.; DeTitta, G.; Caruthers, J. M.; Hodgson, K. O.; Soltis, M.; Zucker, F.; Verlinde, C. L.; Merritt, E. A.; Schoenfeld, L. W.; Hol, W. G. Crystal structure of glyceraldehyde-3-phosphate dehydrogenase from *Plasmodium falciparum* at 2.25 Å resolution reveals intriguing extra electron density in the active site. *Proteins: Struct., Funct., Genet.* **2006**, *62*, 570–577.
- (25) Basore, K.; Cheng, Y.; Kushwaha, A. K.; Nguyen, S. T.; Desai, S. A. How do antimalarial drugs reach their intracellular targets? *Front. Pharmacol.* **2015**, *6*, 91.
- (26) Sonawane, D. P.; Persico, M.; Corbett, Y.; Chianese, G.; Di Dato, A.; Fattorusso, C.; Tagliatalata-Scafati, O.; Taramelli, D.; Trombini, C.; Dhavale, D. D.; Quintavalla, A.; Lombardo, M. New antimalarial 3-methoxy-1,2-dioxanes: optimization of cellular pharmacokinetics and pharmacodynamics properties by incorporation of amino and N-heterocyclic moieties at C4. *RSC Adv.* **2015**, *5*, 72995–73010.
- (27) Lipinski, C. A.; Lombardo, F.; Dominy, B. W.; Feeney, P. J. Experimental and computational approaches to estimate solubility and permeability in drug discovery and development settings. *Adv. Drug Delivery Rev.* **2001**, *46*, 3–26.
- (28) Kirk, K. Membrane transport in the malaria-infected erythrocyte. *Physiol. Rev.* **2001**, *81*, 495–537.